The Scientific Legacy of the 20th Century
Pontifical Academy of Sciences, Acta 21, Vatican City 2011
www.pas.va/content/dam/accademia/pdf/acta21/acta21-rodriguez.pdf

Quantifying the potential impacts of climate change on vegetation diversity at large spatial scales

Megan Konar, Ignacio Rodríguez-Iturbe

1. Introduction

Climate change is likely to be the most significant threat to biodiversity worldwide after 2050 (Strengers *et al.*, 2004). For this reason, quantification of the potential impacts of climate change on biodiversity is urgently needed (Sala *et al.*, 2000; Clark *et al.*, 2001; Botkin *et al.*, 2007). The various features associated with climate change (e.g. temperature, precipitation patterns, CO_2 concentrations, sea level rise, etc.) will likely impact different species in unique and unpredictable ways, making it particularly challenging to model.

It is important to consider biodiversity at the appropriate spatial scale when studying the impact of climate change, since projections of environmental variables under climate change are typically provided as large spatial scales (*Intergovernmental Panel on Climate Change*, 2007). Biodiversity is scale-dependent. In fact, one of the oldest and most well documented patterns in community ecology is the species-area curve, which describes the observed increase in species richness as area increases (Preston, 1962; Rosenzweig, 1995). This relationship has long fascinated ecologists, leading to an extensive literature devoted to the scale dependence of diversity patterns (Currie, 1991; Crawley and Harral, 2001; Hui, 2009). While the increase in the number of species with area is a widely recognized empirical phenomenon, the mechanisms driving this observed relationship are still widely debated in the literature. Since biodiversity is scale-dependent, the spatial scale must be appropriate when coupling biodiversity and climate change models. For this reason, we focus on quantifying the impact of climate change on biodiversity at large spatial scales in this paper.

In this paper, we highlight some recent efforts to quantify the potential impacts of climate change on biodiversity, with a particular emphasis on vegetation driven by hydrologic variables. We focus on the diversity of vegetation in two very different ecosystems. The first is the Mississippi-Missouri River System (MMRS), the largest watershed in North America, comprising 2,980,000 km^2, approximately 40% of the surface area of the continental United States. The second is the Everglades National Park (ENP), encompassing nearly 5,700 km^2, which is comprised of a mosaic of different vege-

tation communities. Hydrology has long been recognized as a driving feature in wetland systems and numerous studies have demonstrated a relationship between hydro-patterns and vegetation communities in the Everglades (Ross *et al.*, 2003; Armentano *et al.*, 2006; Zweig and Kitchens, 2008, 2009). However, the recognition of hydrology as a key driver of vegetation diversity in the MMRS has only recently been shown (Konar *et al.*, 2010).

2. Modeling biodiversity patterns

Many modeling efforts are currently underway to understand and predict the loss of biodiversity. In this paper, we utilize two different, yet complementary, approaches to model vegetation diversity at large spatial scales. For the ENP, we develop a community-distribution model, in which vegetation communities are correlated with hydrological regimes (Todd *et al.*, 2010). Projections of hydrologic variables in the ENP, as given by global climate models, are then used to obtain projections of vegetation communities, assuming that the relationship between vegetation communities and their hydrological niche remains constant in the future (Todd *et al.*, 2011). In the MMRS, we utilize a neutral meta-community model, based on population dynamics, with precipitation as a key driver. Precipitation values are obtained for future scenarios from global climate models, and the impacts on tree diversity patterns are quantified (Konar *et al.*, 2010).

2.1. Vegetation communities in the Everglades National Park

The Everglades National Park (ENP) (shown in Fig. 1, p. 364) encompasses nearly 5,700 km^2 and is a mosaic of different vegetation communities (Gunderson and Loftus, 1993). In total, the park has at least 830 vegetation taxa and includes all of the major habitats found within the larger Everglades ecosystem (Avery and Loope, 1983). Prior to the 1900s, the Everglades was a broad, slowly flowing wetland, originating in Lake Okeechobee and flowing south to the Gulf of Mexico. Flow velocities are often less than 1 cm s^{-1} due to the low slope (3 cm km^{-1}) and vegetative interference. Today, the Everglades is a hydrologically altered landscape due to human action and drainage, with flow controlled through an extensive system of levees, pumps, and canals. Even the ENP, designated as a national park, is impacted by human modification to the hydrology. In this section, we briefly describe the community-distribution model of vegetation in the ENP. The interested reader is referred to Todd *et al.* (2010) for additional details.

The Everglades Depth Estimation Network (EDEN) was used to obtain information on hydrological characteristics across the ENP. Namely, this data

set provides daily water level information for the entire freshwater portion of the Everglades. EDEN data is provided at the scale of 400 m × 400 m, based on over 250 monitoring wells, and covers the entire ENP and beyond. We used this information to calculate the number of hydroperiods in a year, the conditional mean depth of each hydroperiod, the mean duration of a hydroperiod, and the percentage of time inundated. For this analysis, we define a hydroperiod as an individual inundation episode. Our calculations are based on the EDEN data from 2000-2007.

Vegetation data was taken from the Center for Remote Sensing and Mapping Science at the University of Georgia and the South Florida Natural Resources Center (Welch and Madden, 1999). In this study, a 20 m × 20 m grid was laid over the ENP study area, for which the dominant vegetation type was extracted, producing over 5 million vegetation pixels. Since the vegetation and hydrology data are provided as difference scales, a hydrology pixel encompasses 400 vegetation pixels. There are 52 plant communities in the ENP provided by the vegetation database, though 13 vegetation communities comprise greater than 1% of the landscape.

The relationship between a vegetation community and the four hydrological variables was evaluated by extracting all pixels with the same dominant vegetation type and then creating histograms of the hydrologic measures. This allows us to differentiate the vegetation communities based upon their hydrological niches. Plotting the distribution of a vegetation community for a particular hydrologic measure allows us to determine where that community is disproportionately represented. From Fig. 2a (p. 364) it is clear that Muhly Grass was predominantly found in drier locations with a mean depth less than 14 cm that were inundated less than 54% of the time. Bay-Hardwood Scrub, on the other hand, tended to be found in wetter locations, with a clear preference for locations that were most constantly inundated (refer to Fig. 2b, p. 364), while Sawgrass, which is the most abundant vegetation type in the ENP by an order of magnitude, demonstrated indifference to the amount of time that a site was inundated, but tended to be found less frequently at sites with a mean depth between 50 and 80 cm (refer to Fig. 2c, p. 364). Our finding that sawgrass is relatively tolerant to the percent time inundated, but more sensitive to the depth of inundation, is supported by previous studies (Gunderson, 1994).

We believe that this study provides a good representation of the linkages between vegetation and hydrological processes because of the large sample size (>5 million vegetation pixels), the use of mean hydrologic conditions over a long period of record (8 years), and the mapping of dominant vegetation type, rather than every community present, thereby limiting the

chance of a change throughout short periods of time. Fig. 2 (p. 364) supports the contention that many vegetation communities within the ENP are structured on hydrological gradients. While multiple factors are undoubtedly important in determining the presence of a particular vegetation type at a given location in a landscape as diverse and dynamics as the ENP, our results decidedly show that hydrological processes are indeed a major influence structuring vegetation communities. In particular, we found that the percent time inundated and the mean depth of inundation are the major discriminatory variables, supporting the findings of Gunderson (1994).

2.2. Tree species in the Mississippi-Missouri River System

The ecologist Richard Levins (1970) was the first to use the term 'metapopulation' to indicate a set of local populations within a larger system. Several models have applied this concept to the study of extinction processes (Hanski and Gaggiotti, 2004). Recently, metapopulation models, using neutral ecological dynamic, have been shown to accurately characterize large-scale biodiversity characteristics of both fish (Muneepeerakul *et al.*, 2008; Bertuzzo *et al.*, 2009) and trees (Konar *et al.*, 2010). In this section, we briefly describe the model used to characterize tree diversity in the Mississippi-Missouri River System (MMRS), shown in Fig. 3 (p. 365). For further detail, the interested reader is referred to Konar *et al.* (2010).

We implemented a neutral metacommunity model of tree diversity in the MMRS. The 824 DTAs of the MMRS were chosen to represent the local communities of the system. Occurrence data for 231 tree species was compiled for each DTA of the MMRS from the U.S. Forest Service Forest Inventory and Analysis Database. These data were then analyzed for two key biodiversity signatures. First, we consider the distribution of local species richness (LSR). LSR is simply the number of species found in a DTA. The spatial distribution of LSR in the MMRS is shown in Fig. 3 (p. 365), and its corresponding histogram is shown in Fig. 4 (p. 365). The frequency distribution of LSR is bimodal due to the environmental heterogeneity of the MMRS, where species-rich DTAs in the east contribute to the peak around 40-50 species, while those DTAs in the west make up the species-poor peak in the histogram. Second, we consider the species rank-occupancy, the number of DTAs in which a particular species is found as a function of its rank.

To model this system, each local community is assigned a tree habitat capacity (H), defined as the number of 'tree units' that are able to occupy each DTA. A tree unit can be thought of as a subpopulation of trees of the same species. A habitat capacity value is assigned to each DTA that is proportional to the forest cover of that DTA. This is because forest cover

is assumed to be the best determinant of the number of trees that are able to exist within a local community.

The model is based on key population dynamics: birth, death, dispersal, colonization, and diversification. Since the model is neutral, all processes implemented in the model are equivalent for all species. At each time step a randomly selected tree unit dies. Another tree unit is selected to occupy the newly available resources. With probability ν, the immigration rate, the empty spot will be occupied by a tree species that does not currently exist within the system; while, with probability $1-\nu$, the empty spot will be colonized by a species that already exists within the system.

The dispersal process determines how individuals move and how the empty spot will be colonized. Since neutral dynamics operate in the model, the probability that an empty spot is colonized by a certain species is dependent only on the relative abundance of the offspring of that species present at the empty location following the dispersal process.

Tree offspring move through the system based on the dispersal kernel, a mathematical representation of how individuals move. Here, two kernels are used to represent the movement of trees in the MMRS: one for colonization within the system (denoted by the subscript C) and a second for immigration into the system from outside (denoted by the subscript I). The colonization kernel is assumed to take the exponential form and uses the two-dimensional landscape structure: $K_{ij} = C_C \exp(-D_{ij}/\alpha_C)$, where K_{ij} is the fraction of tree offspring produced at DTA j that arrive at DTA i after dispersal; C_C is the normalization constant ($\Sigma_i K_{ij} = 1$); D_{ij} is the shortest distance between DTA i and j measured in 2D space; and α_C is the characteristic dispersal length of colonizing individuals. The immigration kernel allows trees to move across the system boundaries as they would in real life. Immigration across the MMRS boundaries is incorporated into the model by making ν_i, the immigration rate at DTA i, a function of distance to the system boundary and the habitat capacity of the associated boundary DTA, since it is reasonable that immigration would occur more frequently through hospitable environments. The immigration rate is thus calculated as: $\nu_i = C_I H_{bi} exp(-D_{bi}/\alpha_I)$, where H_{bi} and D_{bi} are the habitat capacity of the boundary DTA closest to DTA i and the distance between them, respectively; C_I is the normalization constant ($\Sigma_i \nu_i = \psi$), where ψ is the average number of immigrant species in one generation (defined as the period over which each tree unit dies once on average); and α_I is the characteristic distance travelled by immigrants.

As illustrated in Fig. 4 (p. 365), the model provides an excellent fit to the empirical patterns of tree diversity in the MMRS as well as its sub-regions.

Of key importance, this modeling approach allows for the direct linkage of large-scale biodiversity patterns to environmental forcings (i.e. precipitation). A common point of confusion in the use of neutral models is that they ignore environmental variation. However, we would like to stress that neutral models are able to capture the impact of changing environmental drivers. Individuals in neutral models respond to environmental changes; however, they do so in an equivalent manner.

3. Impacts of climate change

In the previous section, we showed that hydrology structures both vegetation communities and diversity patterns at the ecosystem scale in two very different environments, namely, the Everglades National Park and the Mississippi-Missouri River System. In this section, we briefly describe the potential impacts of climate change on vegetation in both systems. The interested reader is referred to Todd *et al.* (2011) and Konar *et al.* (2010) for additional description and results.

In the ENP, vegetation communities were shown to associate with different hydrological niches. By comparing a vegetation community's relative abundance at given depths and percent time inundated, relative to its system-wide abundance, we have shown that vegetation communities react differently to hydrologic conditions. For example, a community like Sawgrass is able to persist in a variety of hydrologic conditions, while the distribution of a community like Bay-Hardwood Scrub is more narrowly controlled by hydrologic environments. In order to determine the impact of climate change on these vegetation communities, we assume the relationship between the vegetation communities and hydrologic niche remains constant, and project these same hydrologic variables under climate change.

Using our computed changes in hydrologic class frequency and the developed vegetation-hydrology relationship, we predicted the percent cover of individual vegetation communities across the entire ENP. Here, we focus on the changes observed between present conditions and the high emissions climate change scenario, since all emissions scenarios showed a similar impact on vegetation community change. Community changes under the high emissions scenario showed the most extreme departures, so they are presented here for the 'worst-case' scenario.

Recall that there were 13 vegetation communities that individually comprise >1% of the ENP landscape under the current climate scenario. Under the high emissions scenario, this drops to 11 vegetation communities (refer to Table 1). Five communities that had percent coverage greater than 1%

Vegetation Type	Present	High	% Change
Sawgrass	60.68	55.21	-9.0
Mixed Gramminoids	6.55	8.82	34.7
Tall Sawgrass	5.80	2.24	-61.4
Muhly Grass	4.07	10.25	152.0
Spike Rush	2.98	1.38	-53.5
Red Mangrove Scrub	2.16	0.92	-57.4
Bayhead	1.72	0.83	-51.7
Pine Savanna	1.59	5.17	224.3
Willow Shrublands	1.47	1.36	-7.9
Dwarf Cypress	1.45	0.69	-52.1
Bay-Hardwood Scrub	1.44	0.49	-66.1
Brazilian Pepper	1.22	2.50	104.4
Cattail Marsh	1.09	0.29	-73.5
Slash Pine with Hardwoods	0.88	2.96	237.2
Hardwood Scrub	0.71	1.57	121.9
Subtropical Hardwood Forest	0.75	1.43	91.1

Table 1. Percent coverage of dominant vegetation types within Everglades National Park under the present and high emissions scenarios. The percent change of dominant vegetation types between the present and high emissions scenarios are also provided. Only those vegetation types constituting more than one percent of the total landscape are listed. Taken from Todd *et al.* (2011).

under present conditions fell below the 1% threshold (i.e. Red Mangrove Scrub, Bayhead, Dwarf Cypress, Bay-Hardwood Scrub, and Cattail Marsh), while three communities that represented less than 1% of the landscape under present conditions increased above this threshold under climate change (i.e. Slash Pine with Hardwoods, Hardwood Scrub, and Subtropical Hardwood Forest). Under climate change, Sawgrass remained the most dominant vegetation community, though its relative abundance decreased from 60.7% to 55.2%. Other communities showed large decreases in percent cover, such as Cattail Marsh, Bay-Hardwood Scrub, and Tall Sawgrass. In contrast, Slash Pine with Hardwoods, Pine Savanna, Muhly Grass, Hardwood Scrub, and Brazilian Pepper all showed large increases in abundance under climate change.

Thus, changes in the hydrologic landscape under the most extreme emissions scenario led to profound changes in the frequency and distribution of vegetation communities in the ENP. There was a net loss of two vegetation communities under climate change. Some vegetation communities declined under climate change, while some demonstrated a positive reaction to climate change. Specifically, communities that tend to prefer xeric con-

ditions became more numerous, whereas communities that prefer more hydric conditions became more scarce. One surprising finding was that the forecasted drier conditions may allow other vegetation communities to competivitely displace Sawgrass.

For the MMRS system, we showed that a neutral metacommunity model effectively reproduces several characteristic patterns of tree diversity simultaneously when coupled with an appropriate indicator of habitat capacity and dispersal kernel. It is important to highlight that a single climatic variable (i.e. mean annual precipitation, MAP) was used to represent the habitat capacity of trees. Establishing a functional relationship between forest cover and mean annual precipitation allows us to force the model with new values of habitat capacity under climate change and quantify changes in the tree diversity patterns. This is an important step in quantifying the potential impacts of climate change on biodiversity patterns.

Projections of MAP were used to obtain new values of habitat capacity for the 824 DTAs in the MMRS. Specifically, the mean annual precipitation from 2049-2099 was determined for 15 statistically downscaled climate projections from the Coupled Model Intercomparison Project 3 (CMIP3) for the A2 emissions path CMIP3 (2009). The A2 emissions path is the most extreme pathway given by the Intergovernmental Panel on Climate Change (2007). However, recent carbon dioxide emissions are above those in the A2 scenario, indicating that this scenario may be more conservative than initially though, though future emissions remain uncertain (Karl *et al.,* 2009).

A schematic of how new values of habitat capacity were calculated from projections of MAP is provided in Fig. 5 (p. 366). Potential forest cover under the current climate scenario is depicted by points 'A'. To obtain P values under the climate change scenarios, the projected MAP for DTA *i* is located on the graph and the new corresponding potential forest cover is noted. These new values of P are represented on Fig. 5 by points 'B'. This new value of potential forest cover was then used in the equation $H_i = C_H P_i I_i$ to calculate the habitat capacity of DTA *i* under climate change. Both I and C_H are assumed to remain constant under climate change. This ensures that any differences between model realization are due only to climate change.

With these resulting new habitat capacities, we determine how various climate change scenarios are projected to affect tree diversity patterns in the MMRS. Each of the 15 climate change scenarios given by CMIP3 was implemented in the model. Here, the results that pertain to the most dramatic lower (i.e. 'species-poor') and upper (i.e. 'species-rich') bounds in the biodiversity patterns are reported in Fig. 6 (p. 366). Note that the probability of any particular outcome in macrobiodiversity patterns is heavily reliant

on the probabilities associated with the projected precipitation patterns provided by the global climate models. For this reason, the patterns reported here should be interpreted as envelopes of plausible biodiversity scenarios, rather than as predictions of biodiversity outcome.

With the tree diversity patterns under the current climate as a benchmark (i.e. the black line in Fig. 6, p. 366), there is a decrease in the frequency of high diversity local communities and an increase in the frequency of low diversity local communities across all systems in the species-poor scenarios. Additionally, the peaks of the LSR histograms associated with the MMRS and all sub-regions shift leftward, i.e., in the species-poor direction. Of importance, the tail of the rank-occupancy curve exhibits the largest contraction, which is where rare species in the system are represented. In other words, rare species are likely to be disproportionately impacted under climate change, a finding shared with niche-based model Morin and Thuiller (2009).

Tree diversity patterns are impacted more under the species-poor scenarios than under the species-rich scenarios, with the exceptions of the North and Northwest sub-regions, where impacts are of comparable magnitudes under both scenarios. This is due to the changes in the habitat capacities of these regions under both scenarios, as DTAs in these regions are located on the increasing portion of the function (i.e. the blue points in Fig. 5, p. 366), such that increases to MAP translate to increased values of habitat capacity. This is not the case in the the South sub-regions, for example, where increases to MAP do not lead to increased values of habitat capacity, since the function saturates in this region (i.e. note the red points in Fig. 5, p. 366).

Although changes to MAP do not solely determine how the tree diversity patterns will be impacted, it is an important component. The species-poor and species-rich scenarios tend to correspond to those scenarios in which the MAP was among the lowest or the highest, respectively, for a given system. However, there are situations in which this is not the case, such as in the South sub-region, where CNRM-CM3 is classified as the species-poor scenario, even though the average MAP is lowest under the GFDL-CM2.0 model (refer to Table 2).

A map of projected changes to mean local species richness under the species-poor scenario is provided in Fig. 7 (p. 367). Note the decreasing trend in the percentage of species lost from West to East. However, DTAs west of 97.5°W are low-diversity, while those east of 97.5°W are species-rich (similar to the case of fish explored in the previous section). Thus, there is an increasing trend in the absolute number of species lost from West to East. The largest decrease in region-averaged LSR occurs in the South sub-region, where 6.3 species are projected to be lost on average.

Scenario	MMRS	North	Southwest	East	South	Northwest
Current	790.08	831.62	571.38	1177.27	1237.87	432.70
BCCR-BCM2.0	840.73	898.64	515.04	1360.49	1301.49	460.07
CGCM3.1 (T47)	901.58	963.37	584.28	1356.10	1370.95	527.48
CNRM-CM3	778.80	882.67	436.89	1295.90	**1176.41**	440.99
CSIRO-Mk3.0	853.54	918.88	581.37	1292.85	1279.78	489.99
GFDL-CM2.0	711.61	784.22	**382.52**	1203.40	*1062.83*	411.35
GISS-ER	899.59	1032.24	508.99	**1479.87**	1418.20	451.23
INM-CM3.0	709.41	777.85	467.90	*1069.25*	1058.09	412.90
IPSL-CM4	715.84	784.20	477.33	1089.84	1001.62	428.19
MIROC3.2	**654.41**	**684.62**	412.58	1040.21	994.41	**355.29**
ECHO-G	868.32	918.59	646.06	1283.78	1337.44	485.51
ECHAM5/MPI-OM	850.37	911.29	554.26	1339.91	1303.14	463.10
MRI-CGCM2.3.2	868.41	*965.67*	571.59	1316.05	1350.87	480.27
CCSM3	*890.18*	930.47	614.50	1396.40	1358.08	496.96
PCM	887.12	898.73	*644.60*	1335.32	1321.70	*526.24*
UKMO-HadCM3	795.37	824.48	488.05	1297.19	1231.82	437.27

Table 2. Mean annual precipitation (MAP) of the systems considered in this study for the current climate scenario and fifteen climate change scenarios. All values are in mm. Nomenclature of the climate change scenarios follows that of CMIP3. Numbers highlighted in bold indicate the species-poor climate change scenario for a given system, those in italics indicate the species-rich climate change scenario.

Thus, we have quantified the potential impacts of climate change, with hydrologic variables acting as the conduit, on vegetation diversity, both at the community and at the species level. Both models that we implemented are appropriate for use at large spatial scales, an important consideration for climate change impact analysis. One advantage of the neutral model is that it does not assume that the relationship between species and environmental variables remains constant in the future. However, a drawback to the neutral model, is that we are not able to directly map between species in the real world and those in the model, to determine how climate change will impact a particular species, as we are in the community distribution approach. Thus, these modeling approaches are complementary in nature to one another. Both approaches suggest that climate change may dramatically alter key diversity patterns at large spatial scales. These complementary analyses allow us to quantify the potential impacts of climate change on biodiversity, with far reaching implications for conservation biology, restoration efforts, and resource management.

References

Armentano, T., J. Sah, M. Ross, D. Jones, H. Cooley, and C. Smith (2006), Rapid responses of vegetation to hydrological changes in Taylor Slough, Everglades National Park, Florida, USA, *Hydrobiologia*, 569, 293-309, doi:10.1007/s10750-006-0138-8.

Avery, G., and L. Loope (1983), *Plants of the Everglades National Park: A preliminary checklist of vascular plants*, 2nd ed., U.S. Department of the Interior.

Bertuzzo, E.R., R. Muneepeerakul, H.J. Lynch, W.F. Fagan, I. Rodríguez-Iturbe, and A. Rinaldo (2009), On the geographic range of freshwater fish in river basins, *Water Resources Research*, 45.

Botkin, D.B., H. Saxe, M.B. Araujo, R. Betts, R.H.W. Bradshaw, T. Cedhagen, P. Chesson, T.P. Dawson, J.R. Etterson, D. P. Faith, S. Ferrier, A. Guisan, A.S. Hansen, D.W. Hilbert, C. Loehle, C. Margules, M. New, M.J. Sobel, and D.R. B. Stockwell (2007), Forecasting the effects of global warming on biodiversity, *BioScience*, 57 (3), 227-236.

Clark, J.S., S.R. Carpenter, M. Barber, S. Collins, A. Dobson, J.A. Foley, D.M. Lodge, M. Pascual, R.P. Jr., W. Pizer, C. Pringle, W.V. Reid, K.A. Rose, O. Sala, W.H. Schlesinger, D.H. Wall, and D. Wear (2001), Ecological forecasts: An emerging imperative, *Science*, 293, 657-660.

CMIP3 (2009), Statistically Downscaled WCRP CMIP3 Climate Projections, http://gdo-dcp.ucllnl.org/downscaled_cmip3_projections/dcpInterface.html.

Crawley, M.J., and J.E. Harral (2001), Scale dependence in plant biodiversity, *Science*, 291, 864-868.

Currie, D.J. (1991), Energy and large-scale patterns of animal and plant species richness, *The American Naturalist*, 137 (1), 27-49.

Gunderson, L. (1994), Vegetation of the Everglades: determinants of community composition. In: Davis S.M. and Ogden J.C., editors. *Everglades: the ecosystem and its restoration*, 323-340 pp., St. Lucie Press.

Gunderson, L., and W. Loftus (1993), The Everglades. In: Martin W.H., Boyce S.G., Echternacht A.C., editors. *Biodiversity of the Southeastern United States: Lowland terrestrial communities*, 199-255 pp., John Wiley & Sons, Inc.

Hanski, I., and O. Gaggiotti (2004), *Ecology, genetics, and evolution of metapopulations*, Elsevier Academic Press.

Hui, C. (2009), On the scaling patterns of species spatial distribution and association, *Journal of Theoretical Biology*, 261, 481-487.

Intergovernmental Panel on Climate Change (2007), *Climate Change 2007: The Physical Basis*. Contribution of Working Group I to the Fourth Assessment Report of the Intergovernmental Panel on Climate Change, Cambridge University Press.

Karl, T.R., J.M. Melillo, and T.C. Peterson (2009), *Global climate change impacts in the United States*, Cambridge University Press.

Konar, M., R. Muneepeerakul, S. Azaele, E. Bertuzzo, A. Rinaldo, and I. Rodríguez-Iturbe (2010), Potential impacts of precipitation change on large-scale patterns of tree diversity, *Water Resour. Res.*, 46, W11,515.

Morin, X., and W. Thuiller (2009), Comparing niche- and process-based models to reduce prediction uncertainty in species range shifts under climate change, *Ecology*, 90 (5), 1301-1313.

Muneepeerakul, R., E. Bertuzzo, H.J. Lynch, W.F. Fagan, A. Rinaldo, and I. Rodríguez-Iturbe (2008), Neutral metacommunity models predict fish diversity patterns in Mississippi-Missouri basin, *Nature*, 453, 220-222, doi:10.1038/nature06813.

Preston, F. (1962), The canonical distribution of commonness and rarity, *Ecology*, 43 (185-215), 410-432.

Rosenzweig, M.L. (1995), *Species diversity in space and time*, Cambridge University Press.

Ross, M., D. Reed, J. Sah, P. Ruiz, and M. Lewin (2003), Vegetation: environment relationships and water management in Shark Slough, Everglades National Park, *Wetlands Ecol. Manag.*, 11, 291-303.

Sala, O.E., F.S.C. III, J.J. Armesto, E. Berlow, J. Bloomfield, R. Dirzo, E. Huber-Sandwald, L.F. Huenneke, R.B. Jackson, A. Kinzig, R. Leemans, D.M. Lodge, H.A. Mooney, M. Oesterheld, N. L. Poff, M.T. Sykes, B.H. Walker, M. Walker, and D.H. Wall (2000), Global biodiversity scenarios for the year 2100, *Science*, 287, 1770-1774.

Strengers, B., R. Leemans, B. Eickhout, B. de Vries, and A. Bouwman (2004), The land-use projections and resulting emissions in the IPCC SRES scenarios as simulated by the image 2.2 model, *GeoJournal*, 61, 381-393.

Todd, M.J., R. Muneepeerakul, D. Pumo, S. Azaele, F. Miralles-Wilhelm, A. Rinaldo, and I. Rodríguez-Iturbe (2010), Hydrological drivers of wetland vegetation community distribution within Everglades National Park, Florida, *Advances in Water Resources*, 33, 1279-1289.

Todd, M.J., R. Muneepeerakul, F. Miralles-Wilhelm, A. Rinaldo, and I. Rodríguez-Iturbe (2011), Possible climate change impacts on the hydrological and vegetative character of Everglades National Park, Florida, *Ecohydrology*.

Welch, R., and M. Madden (1999), Vegetation map and digital database of South Florida's National Park Lands, final report to the U.S. Department of the Interior, National Park Service, Cooperative Agreement Number 5280-4-9006, Tech. rep., Center for Remote Sensing and Mapping Science, University of Georgia, Athens, GA.

Zweig, C., and W. Kitchens (2008), Effects of landscape gradients on wetland vegetation communities: information for large-scale restoration, *Wetlands*, 28, 1086-96.

Zweig, C., and W. Kitchens (2009), Multi-state succession in wetlands: a novel use of state and transition models, *Ecology*, 90, 1900-9.

Figure 1. Map of the Everglades National Park (ENP) study area. Figure taken from Todd *et al.* (2010).

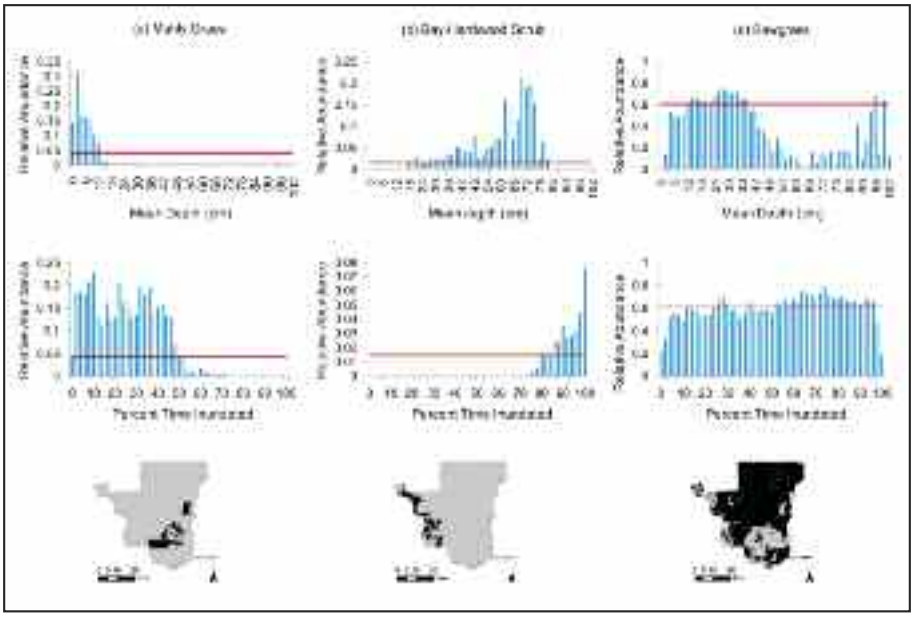

Figure 2. Relative abundance of mean depth, relative abundance of percent time inundated, and spatial distribution of three vegetation types: (a) Muhly grass; (b) Bay-Hardwood scrub; and (c) Sawgrass. The red line indicates the relative abundance of the given vegetation community across the entire landscape. Figure adapted from Todd *et al.* (2010).

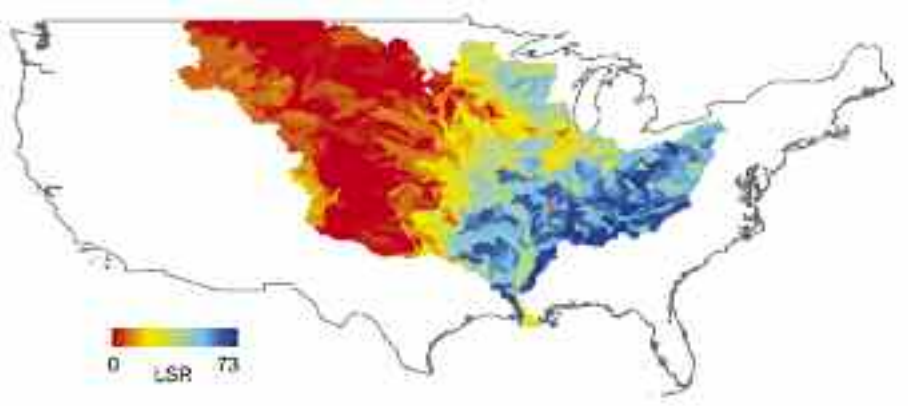

Figure 3. Map of local species richness (LSR) of trees in each direct tributary area (DTA) (that is, at the USGS HUC-8 scale; refer to text) of the MMRS. Taken from Konar *et al.* (2010).

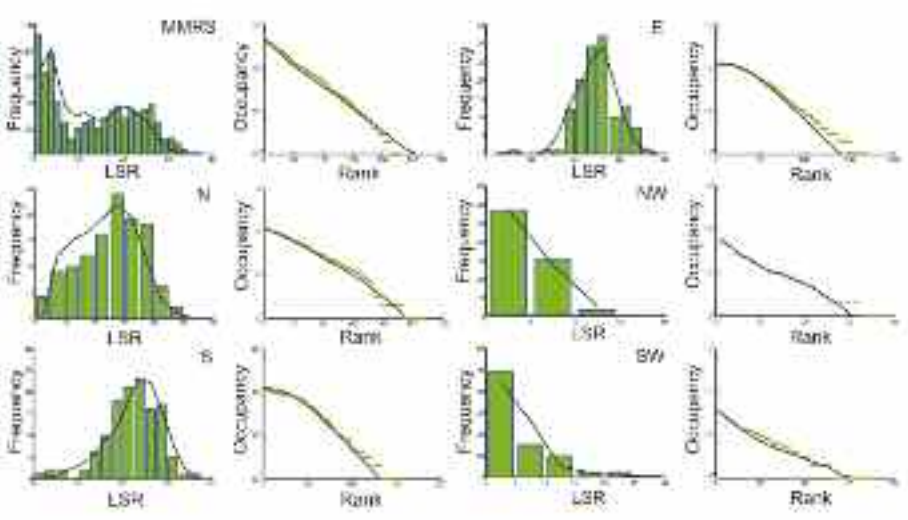

Figure 4. Model fit to empirical patterns of each system. Green shows empirical data; black curves model results. The first and third column illustrate the LSR histogram. The second and fourth column illustrate the rank-occupancy graph. 'MMRS' represents the Mississippi-Missouri River System; 'E' the East subregion; 'N' the North sub-region; 'NW' the Northwest sub-region; 'S' the South sub-region and 'SW' the Southwest sub-region. Refer to Fig. 7 for the spatial extent of each system. Taken from Konar *et al.* (2010).

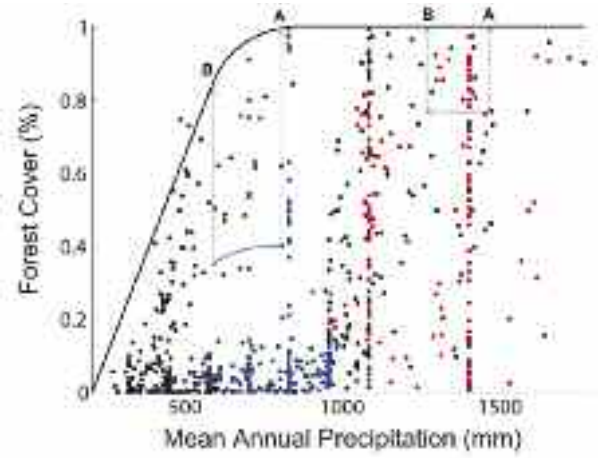

Figure 5. Schematic of how habitat capacity was calculated under climate change. The mean annual precipitation (MAP) for each DTA under every scenario was located on the graph; only data points from the current climate scenario are shown here. The corresponding potential forest cover (Pi) was determined as the upper bound of the function. As an example, points A on the figure indicate the potential forest cover under the current climate scenario, while points B indicate the new potential forest cover under climate change. This new potential forest cover was then multiplied by the forest cover index (Ii) to calculate the habitat capacity under each climate change scenario. This was done for all 824 DTA data points in all 15 climate change scenarios. Blue points indicate DTAs in the North regions; red points the South region; and black points the rest. Taken from Konar *et al.* (2010).

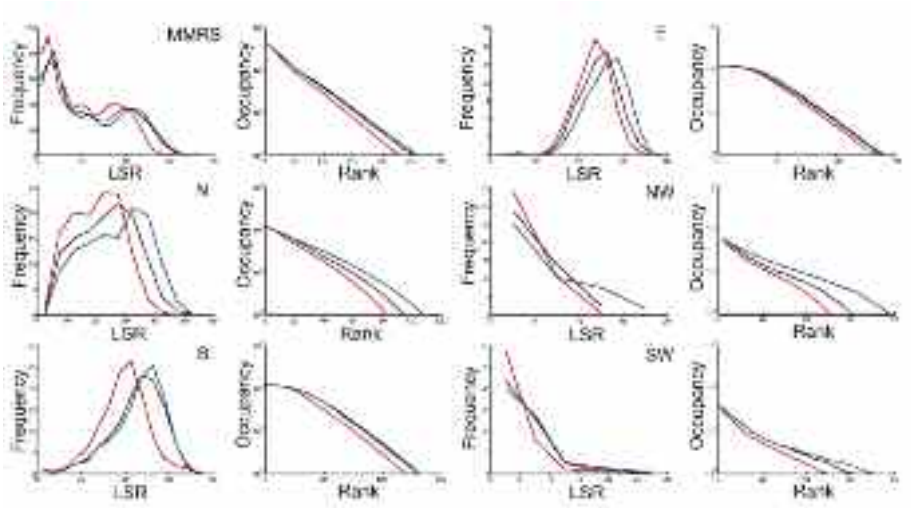

Figure 6. Impact of climate change on the biodiversity patterns of each system. The acroynyms are the same as in Fig. 4. The first and third column illustrate the LSR histogram. The second and fourth column illustrate the rank-occupancy graph. Black curves show model results under the current climate scenario; red curves show the species-poor scenario, and blue curves show the species-rich scenario. Taken from Konar *et al.* (2010).

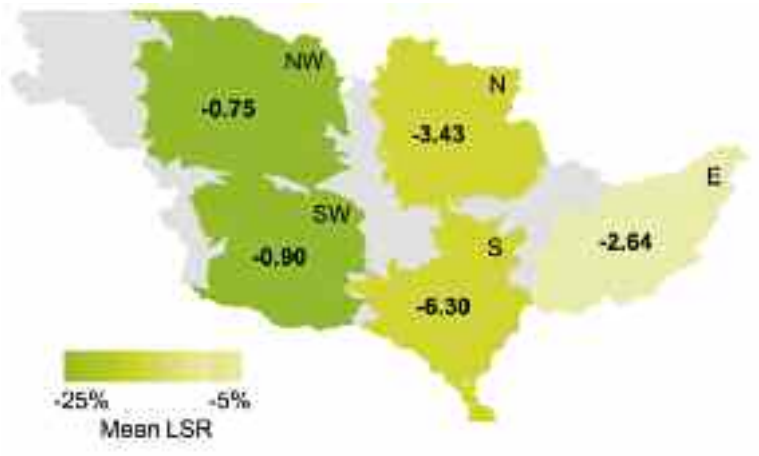

Figure 7. Impact of climate change under the species-poor scenario on region-averaged LSR in sub-regions of the MMRS. The acroynyms are the same as in Fig. 4. Shades of green indicate the percentage change in the region-averaged LSR under climate change, with dark green indicating a higher percentage lost. The general trend is that a higher percentage of species are lost in the west with a decreasing trend to the east. The change per DTA in region-averaged LSR under climate change is indicated for each region by the bold numbers. The species-rich regions east of the 100oW meridian lose more species, though these species represent a smaller percentage of species in these regions. The mean LSR in the South is anticipated to decrease by 6.3 species under climate change, the largest loss of all sub-regions.